Special Issue Article

Journal of Intelligent Material Systems and Structures

Journal of Intelligent Material Systems and Structures
24(18) 2239–2244

DOI: 10.1177/1045389X12469449
jim.sagepub.com
SAGE

Research on ultrafast wavelength conversion device by using tellurite glass

Seiko Mitachi and Yuji Nagahara

Abstract

In the wavelength-division multiplexing network, high-performance optical wavelength converters are desired. This article will report very stable second harmonic generation by using tellurite glasses, second harmonic generation comparison in glass materials, and time-dependent change of second harmonic generation. We obtained 9 times larger second harmonic generation using TeO_2 (60 mol%)–WO_3 (30 mol%)–Bi_2O_3 (10 mol%) than using TeO_2 (60 mol%)–WO_3 (30 mol%)–PbO (10 mol%) glass. This value corresponds to 4.6 times higher than d_{11} constant of Y-cut quartz (0.4 pm/V). We have succeeded permanent poling by measurement of time-dependent change of second harmonic generation because there could not be found second harmonic generation intensity change after 6 months of poling at room temperature, and there was no decay of second harmonic generation intensity after 4 h of heating at 100°C.

Keyword

Fiber optics, non-linear optical glass, wavelength converters

Introduction

In wavelength-division multiplexing photonic networks, high-performance optical wavelength converters are desired. Ferroelectric single crystals such as $LiNbO_3$ have been used to achieve high wavelength conversion efficiency (Asobe et al., 2001; Kintaka et al., 1996; Mizuuchi et al., 1997; Myers et al., 1995). However, single crystals have some restrictions in device fabrication, are relatively expensive, and sometimes experience optical damage. Therefore, new materials with high second-order nonlinear optical properties and introducible quasi-phase matching are required to enable inexpensive and widely usable wavelength converters.

In this study, we investigated tellurite glass systems, which have high optical transmittance over a wide wavelength range (Mitachi et al., 2003) and are expected to have high second-order nonlinear optical properties (Tanaka, 2005; Tanaka et al., 2000). While glass is an optically isotropic body and does not normally exhibit second-order nonlinear optical properties, second-order nonlinearity can be induced by deforming the reversal symmetry with a poling process. If we succeed in forming a quasi-phase matching structure in glass, we expect to achieve an inexpensive and highly efficient wavelength converter by difference frequency generation with a long length waveguide structure. Figure 1 shows the principle of wavelength conversion. A signal light of 1.55 μm (ω_1) is mixed with an excitation light of 0.78 μm (ω_3). They are then added to a quasi-phase matching medium, and a signal light of 1.55 μm (ω_1) is converted into 1.57 μm (ω_2) as shown by

$$\omega_3 - \omega_1 = 1/0.78 - 1/1.55 = 1/1.57 = \omega_2 \quad (1)$$

The polarization inversion pitch, Λ, is decided by

$$\beta\omega_3 - \beta\omega_1 - \beta\omega_2 = 2\pi/\Lambda \quad (2)$$

where β is the propagation constant of an optical axis component when light is propagating in the medium of refractive index n_1 with angle θ, which is expressed as

$$\beta = (2\pi n_1/\lambda)\cos\theta \quad (3)$$

In this article, we report very stable second harmonic generation (SHG) by using tellurite glass. A comparison of SHG in glass materials and the time-dependent changes of SHG are also presented.

Graduate School of Bionics, Computer and Media Sciences, Tokyo University of Technology, Hachioji, Tokyo, Japan

Corresponding author:
Seiko Mitachi, Graduate School of Bionics, Computer and Media Sciences, Tokyo University of Technology, Hachioji, Tokyo 192-0982, Japan.
Email: mitachi@cs.teu.ac.jp

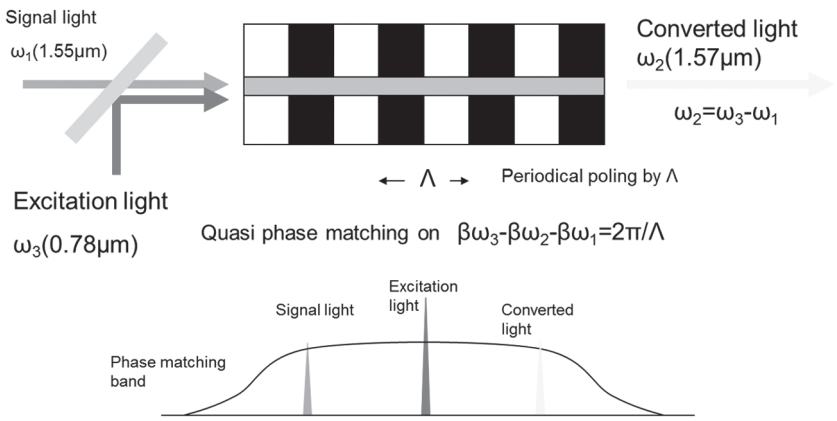

Figure 1. Principle of wavelength conversion element.

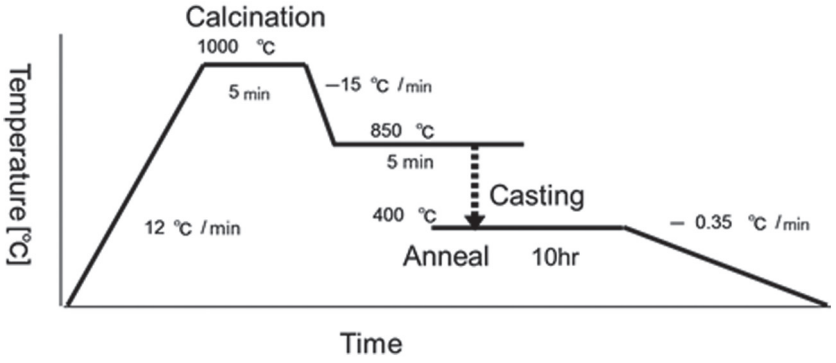

Figure 2. Glass sample preparation process.

Experiments

Glass sample preparation

We prepared two kinds of glass samples, TeO_2 (60 mol%)–WO_3 (30 mol%)–PbO (10 mol%) (T-W-P) and TeO_2 (60 mol%)–WO_3 (30 mol%)–Bi_2O_3 (10 mol%) (T-W-B), by a casting method (Mitachi et al., 2001, 2003). The preparation process is shown in Figure 2. Each material was weighed and mixed in 20 g of mortar and then added to 30 cm^3 of alumina crucible. The crucible was then set in an electric furnace and heated at 1000°C for 5 min and held at 850°C for 5 min for fining. After that the melt was casted into a mold heated at 400°C. After 10 h of annealing, the glass sample was cooled to room temperature in about 20 h. The temperature details are shown in Figure 2. We then cut the samples into rectangular plates (15 mm × 15 mm × 2 mm^t) and optically polished them with a buff finish to obtain rectangles with thickness from 1.0 to 0.33 mm and total sample size 15 mm × 15 mm.

Poling process

We applied thermoelectric field poling to the polished samples by using the equipment shown in Figure 3. A needle electrode was set as positive, and a flat plate electrode of 10 mm × 10 mm was set as negative. A thermocouple was positioned near the samples to control temperature precisely. To avoid oxidation of the electrodes and electrical breakdown, dry nitrogen gas was filled and then flown inside the equipment at a rate of 1.5 L/min. The poling conditions are shown in Table 1. The temperature was raised by 8°/min to 380°C or 400°C. After 3 kV of electric voltage was applied for 40 min in a 5-mm space between two electrodes, temperature was decreased by 5°/min to 50°C, and then the voltage application was stopped.

SHG measurement

We measured SHG intensity by the Maker-fringe method (Jerphagnon et al., 1970) and calculated the second-order optical nonlinear constant by comparing it with Y-cut quartz as a standard sample. Measurement systems were established by yttrium aluminum garnet (YAG) laser, harmonic separators, and laser power control introducing a delay pulse generator to determine the optimum light power condition for eliminating noisy SHG from unnecessary optical elements like optical attenuators (Figure 4).

Table 1. Conditions of thermoelectric field poling.

Sample	Thickness (mm)	Poling temperature (°C)	Voltage (kV)	Poling duration (min)	Distance of electrodes (mm)
T-W-P	0.7	400	3	40	5
T-W-B	0.7	380	3	40	5

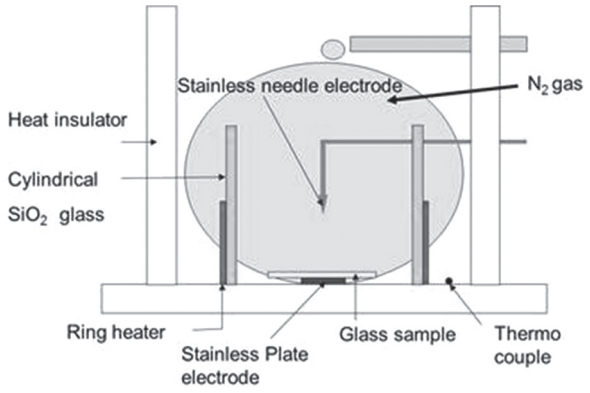

Figure 3. Equipment used for thermoelectric field poling.

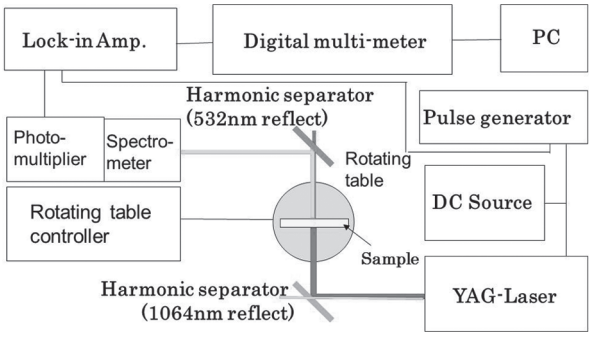

Figure 4. SHG measurement system.
PC: personal computer; DC: direct current; YAG: yttrium aluminum garnet.

Results and discussion

Materials selection

Figure 5 shows the reported glass-forming region of the T-W-P and T-W-B systems (Mitachi et al., 2001, 2003). We chose the composition of T-W-P and T-W-B marked by red circles.

Table 2 shows the reported results of third harmonic generation (THG), absorption edge, and refractive index (n_D) (Mitachi et al., 2001). The glass system with a higher THG is more susceptible to second-order nonlinearity than that with a lower THG because both SHG and THG are the result of the response of the electron clouds of each component element to an electromagnetic wave of light. However, glass is homogeneous and isotropic and generally does not exhibit SHG. We therefore need to break the reversal symmetry, for example, in this case by inducing the orientation inside the glass under thermoelectric poling.

SHG intensity results

The SHG intensity results determined using the Maker-fringe method with the Y-cut quartz as a reference sample are shown in Figure 6. We obtained a bilaterally symmetric pattern by using the measurement system depicted in Figure 4.

Figure 7 shows a comparison of SHG intensity between the T-W-P and T-W-B glass systems measured under the same YAG-laser power condition. We obtained an SHG 9 times larger in T-W-B than in T-W-P. This value for T-W-B corresponds to the 38% of d_{11} constant of the quartz sample (0.22 pm/V).

Poling thickness estimation

The conversion efficiency η between a fundamental wave and a second harmonic wave is expressed as

$$\eta = \frac{P_{2\omega}}{p_\omega} = \frac{8\pi^2}{\varepsilon_0 c\lambda^2}\frac{d^2}{(n_\omega)^2 n_{2\omega}}\frac{p_\omega}{A}L^2\frac{sin^2(\Delta kL/2)}{(\Delta kL/2)^2} \quad (4)$$

where P_ω is the power of a fundamental wave; A is the cross-sectional area of a laser beam; d is the second-order nonlinear optical constant; n_ω and $n_{2\omega}$ are the refractive indices of the fundamental wave and the second harmonic wave, respectively; Δk is the phase shifting; and L is the crystal length. In general, to obtain a higher conversion efficiency η, Δk should be lower, materials with higher d should be used, P_ω/A should be higher by laser light beam focusing, and crystal length L should be long if phase matching is done.

We measured the SHG of samples under the same conditions with thicknesses of 1.0, 0.75, 0.7, 0.5, and 0.33 mm. Results are shown in Table 3.

By formula (4), if phase matching is achieved, the SHG intensity should depend on the square of sample thickness L (crystal length). Figure 8 shows the relationship between SHG intensity and sample thickness.

However, we did not observe dependency on L^2; the SHG intensities were almost completely alike in every sample thickness within an experimental error range. This indicates that there was a problem with the phase matching. Therefore, we could not estimate poling thickness from these results.

Second-order nonlinear optical constant estimation

The second-order nonlinear optical constant of Y-cut quartz is $d_{11} = 0.4$ pm/V. The second-order nonlinear

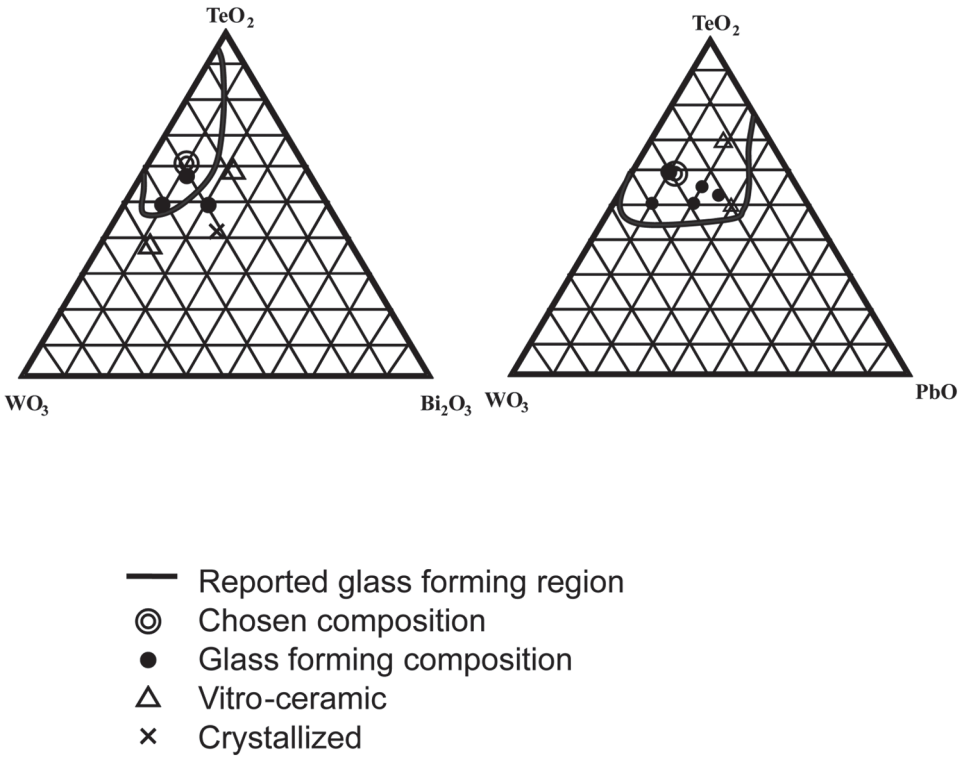

Figure 5. Glass-forming region of TeO_2–WO_3–PbO and TeO_2–WO_3–Bi_2O_3 systems.
Source: Mitachi et al. (2003).

Table 2. Third-order nonlinear optical properties and absorption edge of tellurite glasses.

Composition (mol%)		Refractive index (n_D)	Absorption edge λ_0 (nm)	$X^{(3)}$ ($\times 10^{-12}$ esu)
TeO_2–WO_3–PbO	60–30–10	2.2	397	0.79
TeO_2–WO_3–PbO	60–30–10	2.114	397	0.71
TeO_2–WO_3–Bi_2O_3	60–30–10	2.2	408	1.6
TeO_2–WO_3–TiO_2	62.5–32.5–5	2.2	391	2.2
TeO_2–WO_3–PbO	55–25–20	2.2	398	0.59
TeO_2–WO_3–Nb_2O_5	80–10–10	2.2	393	0.28
TeO_2–WO_3–Bi_2O_3	50–30–20	2.2	404	0.63
TeO_2–WO_3–La_2O_3	55–25–20	2.2	375	0.3
TeO_2–WO_3–Ta_2O_5	80–15–5	2.2	387	0.53
TeO_2–WO_3–La_2O_3	60–30–10	2.2	385	0.88
TeO_2–WO_3–La_2O_3	60–30–10	2.093	385	0.77

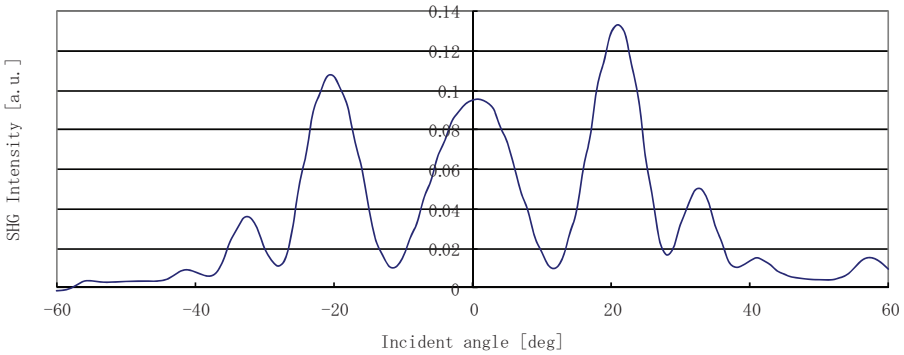

Figure 6. Maker-fringe pattern for Y-cut quartz as a reference sample.
SHG: second harmonic generation.

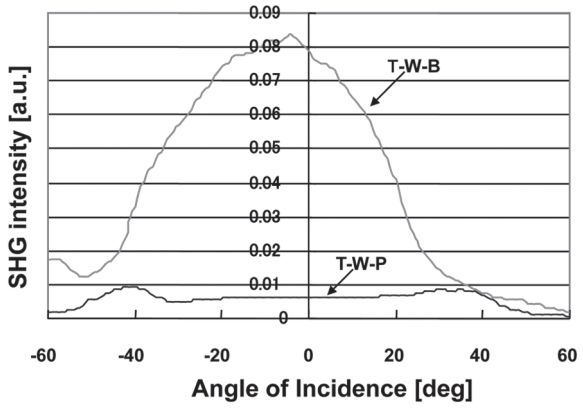

Figure 7. Comparison of SHG intensity between T-W-P and T-W-B glass systems (sample thickness: 0.33 mm).
T-W-P: TeO_2–WO_3–PbO; T-W-B: TeO_2–WO3–Bi_2O_3.

Table 3. SHG intensity for poled glass samples.

Sample	Sample thickness (mm)	SHG intensity (a.u.)
T-W-B_{-5}	0.70	0.0835
T-W-B_{-C2}	0.75	0.0399
T-W-B_{-C3}	0.50	0.1127
T-W-B_{-D2}	0.50	0.0779
T-W-B_{-D3}	0.33	0.0887
T-W-B_{-E1}	0.50	0.0764
T-W-B_{-G1}	1.0	0.0620
T-W-B_{-F2}	1.0	0.0595
T-W-B_{-F3}	1.0	0.0858

SHG: second harmonic generation; T-W-B: TeO_2 (60 mol%)–WO_3 (30 mol%)–Bi_2O_3 (10 mol%).
Sample suffixes are for experimental differentiation.

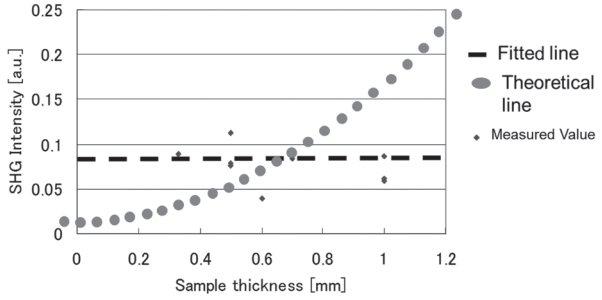

Figure 8. Relationship between SHG intensity and sample thickness in T-W-B.
SHG: second harmonic generation; T-W-B: TeO_2–WO_3–Bi_2O_3.

optical constants (SHG intensity) for the poled glass samples were calculated using this value and the peak ratio of the Maker-fringe pattern between the glass samples and the quartz.

Under the assumption that the entire sample has been poled, we performed the calculation for the 0.33-mm-thick sample, which had shown promise for having the highest SHG value. As shown in Figures 7 and 8, the peak of the fringe pattern was 0.0887 a.u. for T-W-B with a thickness of 0.33 mm and 0.2607 a.u. for the quartz with a thickness of 1 mm. From formula (4), the second-order nonlinear optical constant, d_{sample}, for the poled glass sample is expressed as formula (5) if phase matching is achieved

$$d_{sample} = \frac{d_{quartz}\, L_{quartz}}{L_{sample}} \sqrt{\frac{P_{sample}}{P_{quartz}}} \tag{5}$$

As indicated in Figure 8, phase matching was not achieved, so the second-order nonlinear optical constant, d_{sample}, for the poled glass sample is expressed as

$$d_{sample} = \frac{d_{quartz}\, Lc_{quartz}}{Lc_{sample}} \sqrt{\frac{P_{sample}}{P_{quartz}}} \tag{6}$$

where d_{sample} and d_{quartz} are the second-order nonlinear optical constants, Lc_{sample} and Lc_{quartz} are the coherence lengths, and P_{sample} and P_{quartz} are the SHG intensities for the poled glass sample and the quartz, respectively. Lc_{sample} is calculated from

$$Lc = \lambda/4(n_{2\omega} - n_{2\omega}) \tag{7}$$

The calculated Lc_{quartz} is 20.65 μm, and Lc_{sample} can be analyzed as 2.95 μm by the refractive index dispersion data for T-W-P as $n_{\omega(1064\ nm)}$ is 2.05 and $n_{2\omega(532\ nm)}$ is 2.14. On the assumption that the Lc_{sample} of T-W-B can be approximated by the Lc_{sample} of T-W-P, the second-order nonlinear optical constant derived from formula (6) for T-W-B_{-D3} is $d_{33} = 1.63$ pm/V and for T-W-B_{-C3} is $d_{33} = 1.84$ pm/V. The latter is 4.6 times higher than the $d_{11} = 0.4$ pm/V for Y-cut quartz. According to a previously reported result of X-ray analysis (Tajima and Mitachi, 2006), the actual poled thickness seems to be around several micrometers (derived by Scherrer's equation). Similarly, in this study, both superficial parts seem to be poled, whereas the central region is not.

T-W-B_{-E1} with a thickness of 500 μm showed a SHG intensity of 0.076 a.u. before polishing. After polishing a thickness of 180 μm, this intensity decreased to 0.0433 a.u. After various estimations, we concluded that T-W-B_{-E1} has a structure of one nonpoled layer sandwiched by two poled layers.

Permanent poling

We measured the time-dependent change of the SHG intensity of T-W-B at room temperature (Figure 9) and at 100°C (Figure 10). As the figures indicate, our permanent poling appears to be completely successful, because there was no change to SHG intensity after 6 months of poling at room temperature and there was no decay of SHG intensity after 4 h of heating at 100°C.

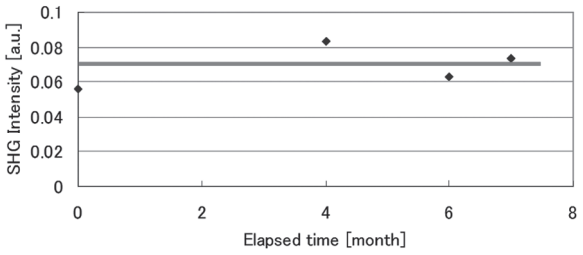

Figure 9. Time-dependent change of SHG intensity of T-W-B at room temperature.
SHG: second harmonic generation; T-W-B: TeO_2–WO_3–Bi_2O_3.

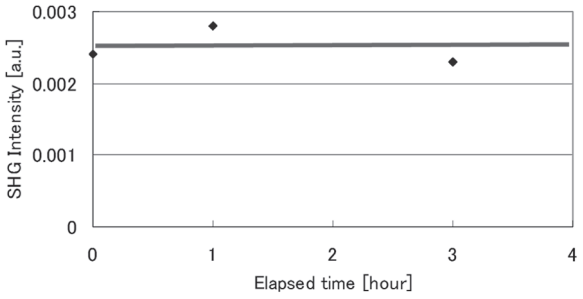

Figure 10. Time-dependent change of SHG intensity of T-W-B at 100°C.
SHG: second harmonic generation; T-W-B: TeO_2–WO_3–Bi_2O_3.

Former studies have shown that the SHG intensity of poled tellurite glass was decayed to 7/10 after 3 h and to 3/10 after 15 h (Tanaka, 2005; Tanaka et al., 2000) at room temperature, apparently because the Na^+ ion migrated from the electrode cover glass to the sample tellurite glass. This is the cause of SHG decay. We were able to achieve almost permanent poling by performing actual poling in a T-W-B system whose constituent elements were moved and fixed by thermoelectric poling near the glass transition temperature.

For our future work, in order to estimate the second-order nonlinear optical constant precisely, we need to measure the poling thickness properly. After poling and SHG intensity measurements, ablation with an accuracy to the micrometer order should be done for each side of the surface periodically until SHG reaches zero or half and then the pole thickness should be estimated.

By optimizing the poling duration and polarization control, we should be able to improve the SHG intensity of the poled glass samples. We are also now trying to form periodic poling structure inside these samples.

Funding

This research was partially supported by the Ministry of Education, Science, Sports and Culture of Japan, Grant-in-Aid for Scientific Research (C), 14550307, 2002-2005.

References

Asobe M, Tadanaga O, Yanagawa T, et al. (2001) Reducing photorefractive effect in periodically poled ZnO- and MgO-doped LiNbO3 wavelength converters. *Applied Physics Letters* 78: 3163–3165.

Jerphagnon J and Kurtz SK (1970) Maker fringes: a detailed comparison of theory and experiment for isotropic and uniaxial crystals. *Journal of Applied Physics* 41(4): 1667–1681.

Kintaka K, Fujiwara M, Suhara T, et al. (1996) High efficiency $LiNbO_3$ waveguide second-harmonic generation devices with ferroelectric- domain-inverted gratings fabricated by applying voltage. *Journal of Lightwave Technology* 14(3): 462–468.

Mitachi S, Isozaki T and Hosaka K (2003) Third-order optical non-linearity of tellurite glass. In: *EUROMAT 2003*, paper no. A3–58. 1–5 September 2003, Lausanne. European Congress and Exhibition on Advanced Materials and Process.

Mitachi S, Kanbara H and Suzuki H (2001) *Third-order optical nonlinearities of tellurite glass*. Technical Report of IEICE. OPE2001-132, pp. 77–82. 23 January 2002, Tokyo. The Institute of Electronics, Information, and Communication Engineers.

Mizuuchi K, Ohta H, Yamamoto K, et al. (1997) Second-harmonic generation with a high-index-clad waveguide. *Optics Letters* 22: 1217–1219.

Myers LE, Eckardt RC, Fejer MM, et al. (1995) Quasi-phase-matched optical parametric oscillators in bulk periodically poled $LiNbO_3$. *Journal of the Optical Society of America B: Optical Physics* 12: 2102–2116.

Tajima Y and Mitachi S (2006) Examination of the relation between the internal atomic periodicity in the poled tellurite glasses and their SHG by X-ray diffraction analysis. Extended Abstracts (53rd Spring Meeting, 2006) No. 2: 956, 22–26 March2006. The Japan Society of Applied Physics and Related Societies.

Tanaka K (2005) Second-order optical nonlinearity and magnetic order in disordered oxides. *Journal of the Ceramic Society of Japan* 113(8): 501–508.

Tanaka K, Narazaki A and Hirao K (2000) Large optical second-order nonlinearity of poled WO_3-TeO_2 glass. *Optics Letters* 25(4): 251–253.